Environ Sci Pollut Res (2017) 24:3539–3549
DOI 10.1007/s11356-016-8017-y

RESEARCH ARTICLE

A model for determination of operational conditions for successful shortcut nitrification

Xiaoguang Liu [1] · **Mingu Kim** [2] · **George Nakhla** [1,2]

Received: 11 August 2016 / Accepted: 28 October 2016 / Published online: 23 November 2016

Abstract Accumulation of nitrite in shortcut nitrification is influenced by several factors including dissolved oxygen concentration (DO), pH, temperature, free ammonia (FA), and free nitrous acid (FNA). In this study, a model based on minimum dissolved oxygen concentration (DO_{min}), minimum/maximum substrate concentration (S_{min} and S_{max}), was developed. The model evaluated the influence of pH (7–9), temperature (10–35 °C), and solids retention time (SRT) (5 days–infinity) on MSC values. The evaluation was conducted either by controlling total ammonium nitrogen (TAN) or total nitrite nitrogen (TNN), concentration at 50 mg N/L while allowing the other to vary from 0 to 1000 mg N/L. In addition, specific application for shortcut nitrification-anammox process at 10 °C was analyzed. At any given operational condition, the model was able to predict if shortcut nitrification can be achieved and provide the operational DO range which is higher than the DO_{min} of AOB and lower than that of NOB. Furthermore, experimental data from different literature studies were taken for model simulation and the model prediction fit well the experiment. For the Sharon process, model prediction with default kinetics did not work but the model could make good prediction after adjusting the kinetic values based on the Sharon-specific kinetics reported in the literature. The model provides a method to identify feasible combinations of pH, DO, TAN, TNN, and SRT for successful shortcut nitrification.

Keywords Ammonia oxidation bacteria (AOB) · Nitrite oxidation bacteria (NOB) · Shortcut nitrification · Minimum dissolved oxygen · Temperature · pH · Modeling prediction

Abbreviations

AOB	Ammonia-oxidizing bacteria
BNR	Biological nitrogen removal
CSTR	Continuous stirred-tank reactor
DO	Dissolved oxygen concentration
DO_{min}	Minimum DO concentration
FA	Free ammonia
FNA	Free nitrous acid
MSC	Minimum/maximum substrate concentration
NOB	Nitrite-oxidizing bacteria
S_{min}	Minimum substrate concentration
S_{max}	Maximum substrate concentration
SRT	Solids retention time
TAN	Total ammonium nitrogen
TNN	Total nitrite nitrogen

Introduction

Conventional biological nitrogen removal (BNR) consists of two successive steps: autotrophic nitrification

Responsible editor: Marcus Schul

Electronic supporting information (ESI): DO data for nitrite accumulation and model derivation.

Electronic supplementary material The online version of this article (doi:10.1007/s11356-016-8017-y) contains supplementary material, which is available to authorized users.

✉ George Nakhla
gnakhla@uwo.ca

[1] Department of Civil and Environmental Engineering, University of Western Ontario, Spencer Engineering Building #3037, London, ON N6A 5B9, Canada

[2] Department of Chemical and Biochemical Engineering, University of Western Ontario, London, ON N6A 5B9, Canada

and heterotrophic denitrification. Nitrification consists of two steps: ammonia is first oxidized to nitrite by ammonia-oxidizing bacteria (AOB), and then nitrite is oxidized to nitrate by nitrite-oxidizing bacteria (NOB). From a biochemical perspective, AOB utilize ammonium (NH_4^+-N) as their electron donor and NOB utilize nitrite (NO_2^-) as electron donor. Both AOB and NOB utilize dissolved oxygen (DO) as their electron acceptor, suggesting that a competition for DO between AOB and NOB exists in nitrification systems. Shortcut nitrification/denitrification and shortcut nitrification/anammox are two promising technologies to replace conventional biological nitrogen removal (BNR) (Guo et al. 2009; Van Loosdrecht and Jetten 1998). The benefits of shortcut nitrification processes include lower oxygen and carbon requirements (Beccari et al. 1983; Turk and Mavinic 1987; van Kempen et al. 2001). Enrichment of AOB and washout or inhibition of NOB are important for realizing the partial nitrification process.

When competing for DO, NOB are often at a disadvantage due to their higher dissolved oxygen half-saturation coefficients. Thus, DO control has been adopted by many researchers to achieve shortcut nitrification. However, DO concentrations for achieving stable shortcut nitrification varied in different studies, as shown in Table 1 of the supporting information (SI). As apparent from SI-Table 1, DO values range from 0.16 to 5 mg DO/L. The wide differences in operational DO concentrations resulted directly from the changes in pH, free ammonia (FA), free nitrous acid (FNA), and temperature, as well as the type of system (attached growth or suspended growth). Thus, optimization of DO concentration at any given operational conditions such as pH, FA, FNA, temperature is critical for the design and operation of a successful shortcut nitrification system.

In this study, we developed a mathematical model proposing the concept of the minimum/maximum substrate (MSC) concentrations to include oxygen limitations and the effect of pH, FA and FNA, temperature, and SRT at a given ambient TNN and TAN concentration. The choice of free ammonia as the AOB substrate is rationalized by Hellinga et al. (1999) and Van Hulle et al. (2007), who demonstrated from batch tests that NH_3 rather than NH_4^+ is the actual substrate, which is also supported by the fact that biomass actually can only transport the uncharged NH_3 over its membrane (Anthonisen et al. 1976). The model was also validated with data from the literature.

Methodology

General MSC equation

S_{min} is the minimum substrate concentration to support steady-state biomass (Rittmann and McCarty 1980; Rittmann and McCarty 2001). S_{min} and DO_{min} can be derived from the Monod equation as Eqs. 1 and 2, respectively (Rittmann and McCarty 2001).

$$S_{min} = K_s \times \frac{b}{\frac{\mu_{max} \times DO}{DO + K_O} - b} \quad (1)$$

$$DO_{min} = K_O \times \frac{b}{\frac{\mu_{max} \times S}{S + K_S} - b} \quad (2)$$

S_{min} refers to the minimum electron donor. K_s and K_o are the Monod half-saturation concentrations for the electron donor (S) and electron acceptor (DO), respectively; μ_{max} is the maximum growth rate and b is the endogenous decay rate.

MSC equation for AOB

In this study, by adopting free ammonia as substrate, Eqs. 1 and 2 are converted to Eqs. 3 and 4.

$$FA_{min} = K_{FA} \times \frac{b}{\frac{\mu_{max} \times DO}{DO + K_O} - b} \quad (3)$$

$$DO_{min} = K_O \times \frac{b}{\frac{\mu_{max} \times FA}{FA + K_{FA}} - b} \quad (4)$$

In which K_{FA} is the Monod half-saturation rate concentration for FA.

MSC equation for NOB

In this study, TNN is chosen as the substrate for NOB (Boon and Laudelout 1962; Park and Bae 2009). Eqs. 1 and 2 are converted to Eqs. 5 and 6:

$$TNN = K_{TNN} \times \frac{b}{\frac{\mu_{max} \times DO}{DO + K_O} - b} \quad (5)$$

$$DO_{min} = K_O \times \frac{b}{\frac{\mu_{max} \times TNN}{TNN + K_{TNN}} - b} \quad (6)$$

In which K_{TNN} is the Monod half-saturation concentration for TNN.

Effect of pH

The pH can influence nitrification directly by changing the enzymatic reaction mechanism (Park et al. 2007; Van Hulle et al. 2007) and indirectly by changing the concentrations of FA and FNA, which inhibit AOB and NOB (Hellinga et al. 1999; Park and Bae 2009; Van Hulle et al. 2007).

The direct pH effect on the maximum specific substrate utilization rate of AOB or NOB can be captured by the empirical bell-shaped Eq. 7 (Park et al. 2007):

$$q = \frac{q_{max}}{2} \times \left\{1 + \cos\left[\frac{\pi}{w} \times \left(\mathrm{pH}-\mathrm{pH}_{opt}\right)\right]\right\} \quad \left(\left|\mathrm{pH}-\mathrm{pH}_{opt}\right| < w\right) \tag{7}$$

q and q_{max} are, respectively, the maximum specific substrate utilization rate at a given pH and at the optimal pH. w is the pH range within which the q is larger than one-half of q_{max}.

Since the biomass yield is a constant, μ is also affected by pH similar to q:

$$\mu = \frac{\mu_{max}}{2} \times \left\{1 + \cos\left[\frac{\pi}{w} \times \left(\mathrm{pH}-\mathrm{pH}_{opt}\right)\right]\right\} \tag{8}$$

μ is the maximum specific substrate utilization rate at a given pH.

FA and FNA, both of which inhibit AOB and NOB, are influenced by pH. FA and FNA concentrations can be calculated based on pH and TAN or TNN concentration (Anthonisen et al. 1976; Park and Bae 2009).

$$\mathrm{FA} = \frac{17}{14} \times \frac{\mathrm{TAN} \times 10^{\mathrm{pH}}}{\exp\left(\frac{6344}{273+T}\right) + 10^{\mathrm{pH}}} \tag{9}$$

$$\mathrm{FNA} = \frac{47}{14} \times \frac{\mathrm{TNN}}{\exp\left[\left(\frac{-2300}{273+T}\right) \times 10^{\mathrm{pH}}\right] + 1} \tag{10}$$

where T is temperature (°C).

Given that FA is the substrate for AOB and FNA is not a substrate for AOB, the inhibition of FA and FNA may potentially be modeled by the following substrate inhibition model (Metcalf&Eddy 2014; Vadivelu et al. 2006) and non-substrate inhibition model (Hellinga et al. 1999), as shown below in Eqs. 11 and 12, respectively.

$$\mu = \mu_{max} \times \frac{\mathrm{DO}}{\mathrm{DO}+K_O} \times \frac{\mathrm{FA}}{K_{FA} + \mathrm{FA} + \frac{\mathrm{FA}^2}{K_{IFA}}} \tag{11}$$

$$\mu = \mu_{max} \times \frac{\mathrm{DO}}{\mathrm{DO}+K_O} \times \frac{\mathrm{FA}}{\mathrm{FA}+K_{FA}} \times \frac{K_{IFNA}}{K_{IFNA}+\mathrm{FNA}} \tag{12}$$

Thus, integrating the direct and indirect effects of pH on AOB yields:

$$\mu_{obs} = \frac{\mu_{max}}{2} \times \left\{1 + \cos\left[\frac{\pi}{w} \times \left(\mathrm{pH}-\mathrm{pH}_{opt}\right)\right]\right\} \times \frac{\mathrm{DO}}{\mathrm{DO}+K_O} \times \frac{\mathrm{FA}}{K_{FA} + \mathrm{FA} + \frac{\mathrm{FA}^2}{K_{IFA}}} \times \frac{K_{IFNA}}{K_{IFNA}+\mathrm{FNA}} \tag{13}$$

K_{IFA} and K_{IFNA} are the inhibition concentrations for FA and FNA on AOB. μ_{obs} is the observed specific biomass growth rate.

A non-substrate inhibition model was adopted for FA inhibition of NOB as FA is not a substrate for NOB. The model by Boon and Laudelout (1962) was chosen to describe the FNA inhibition of NOB. Thus, integrating the direct and indirect effects of pH on NOB yields the following:

$$\mu_{obs} = \frac{\mu_{max}}{2} \times \left\{1 + \cos\left[\frac{\pi}{w} \times \left(\mathrm{pH}-\mathrm{pH}_{opt}\right)\right]\right\} \times \frac{\mathrm{DO}}{\mathrm{DO}+K_O} \times \frac{\mathrm{TNN}}{(K_{TNN}+\mathrm{TNN})\left(1+\frac{\mathrm{FNA}}{K\ddot{E}_{IFNA}}\right)} \times \frac{K'_{IFA}}{K'_{IFA}+\mathrm{FA}} \tag{14}$$

K'_{IFA} and K'_{IFNA} are the inhibition concentration for FA and FNA on NOB.

Effect of temperature

The Monod maximum growth rate (μ_{max}), the half-saturation concentration (K_S), and the endogenous decay rate (b) were adjusted for temperature:

$$\mu_{max} = \mu_{max20} \times \theta_{\mu}^{T-20} \tag{15}$$

$$K_S = K_{S20} \times \theta_{K_S}^{T-20} \tag{16}$$

$$b = b_{20} \times \theta_b^{T-20} \tag{17}$$

where T is temperature (°C); θ is the temperature coefficient.

SRT effect

The effect of SRT on the MSC equations is shown in Eq. 18:

$$\mu_{max} \times \frac{DO}{K_O + DO} \times \frac{S}{S + K_S} - b - \frac{1}{SRT} = 0 \tag{18}$$

Integration of effects

DO_{min} equations for AOB and NOB are shown in Eqs. 19 and 20, respectively.

$$DO_{min} = \frac{\left(b_{20} \times \theta_b^{T-20} + \frac{1}{SRT}\right) \times K_o}{\frac{\frac{\mu_{max20} \times \theta_{\mu}^{T-20}}{2} \times \left\{1 + \cos\left[\frac{\pi}{w} \times \left(pH - pH_{opt}\right)\right]\right\}}{\left(1 + \frac{FNA}{K_{IFNA}}\right) \times \left(1 + \frac{K_{FA20} \times \theta_{K_{FA}}^{T-20}}{FA} + \frac{FA}{K_{IFA}}\right)} - b_{20} \times \theta_b^{T-20} - \frac{1}{SRT}} \text{ for AOB} \tag{19}$$

$$DO_{min} = \frac{\left(b_{20} \times \theta_b^{T-20} + \frac{1}{SRT}\right) \times K_o}{\frac{\frac{\mu_{max20} \times \theta_{\mu}^{T-20}}{2} \times \left\{1 + \cos\left[\frac{\pi}{w} \times \left(pH - pH_{opt}\right)\right]\right\}}{\left(1 + \frac{FNA}{K\ddot{E}_{IFNA}}\right) \times \left(1 + \frac{FA}{K\ddot{E}_{IFA}}\right) \times \left(1 + \frac{K_{TNN20} \times \theta_{K_{TNN}}^{T-20}}{TNN}\right)} - b_{20} \times \theta_b^{T-20} - \frac{1}{SRT}} \text{ for NOB} \tag{20}$$

FA_{min} and FA_{max} for AOB and TNN_{min} and TNN_{max} for NOB can be calculated from Eqs. 21–24, respectively, since FA for AOB and TNN for NOB have two limiting values with FA and FNA inhibition. The lower limiting value (FA_{min} or TNN_{min}) has the same meaning as the traditional S_{min}, i.e., the minimum substrate concentration to support steady-state biomass while the higher value (FA_{max} or TNN_{max}) represents the maximum substrate concentration able to sustain steady-state biomass, above which inhibition by FA or FNA will lead to wash out of AOB or NOB.

For AOB,

$$FA_{min} = \frac{\frac{\mu_{max20} \times \theta_{\mu}^{T-20}}{2} \times \left\{1 + \cos\left[\frac{\pi}{w} \times \left(pH - pH_{opt}\right)\right]\right\} \times DO}{\left(1 + \frac{FNA}{K_{IFNA}}\right) \times (K_O + DO)} - b_{20} \times \theta_b^{T-20} - \frac{1}{SRT} - \sqrt{\left(\frac{\frac{\mu_{max20} \times \theta_{\mu}^{T-20}}{2} \times \left\{1 + \cos\left[\frac{\pi}{w} \times \left(pH - pH_{opt}\right)\right]\right\} \times DO}{\left(1 + \frac{FNA}{K_{IFNA}}\right) \times (K_O + DO)} - b_{20} \times \theta_b^{T-20} - \frac{1}{SRT}\right)^2 - 4 \times \frac{\left(b_{20} \times \theta_b^{T-20} + \frac{1}{SRT}\right)^2 \times K_{FA20} \times \theta_{K_{FA}}^{T-20}}{K_{IFA}}}}{2 \times \left(b_{20} \times \theta_b^{T-20} + \frac{1}{SRT}\right) \times \frac{1}{K_{IFA}}} \tag{21}$$

$$FA_{max} = \frac{\frac{\mu_{max20} \times \theta_{\mu}^{T-20}}{2} \times \left\{1 + \cos\left[\frac{\pi}{w} \times \left(pH - pH_{opt}\right)\right]\right\} \times DO}{\left(1 + \frac{FNA}{K_{IFNA}}\right) \times (K_O + DO)} - b_{20} \times \theta_b^{T-20} - \frac{1}{SRT} + \sqrt{\left(\frac{\frac{\mu_{max20} \times \theta_{\mu}^{T-20}}{2} \times \left\{1 + \cos\left[\frac{\pi}{w} \times \left(pH - pH_{opt}\right)\right]\right\} \times DO}{\left(1 + \frac{FNA}{K_{IFNA}}\right) \times (K_O + DO)} - b_{20} \times \theta_b^{T-20} - \frac{1}{SRT}\right)^2 - 4 \times \frac{\left(b_{20} \times \theta_b^{T-20} + \frac{1}{SRT}\right)^2 \times K_{FA20} \times \theta_{K_{FA}}^{T-20}}{K_{IFA}}}}{2 \times \left(b_{20} \times \theta_b^{T-20} + \frac{1}{SRT}\right) \times \frac{1}{K_{IFA}}} \tag{22}$$

For NOB,

$$\mathrm{TNN_{min}} = \frac{\frac{\mu_{max20}\times\theta_{\mu}^{T-20}\times \mathrm{DO}}{\left(1+\frac{\mathrm{FA}}{K\ddot{\boldsymbol{\epsilon}}_{\mathrm{IFA}}}\right)\times(K_{\mathrm{O}}+\mathrm{DO})} - \left(b_{20}\times\theta_{b}^{T-20}+\frac{1}{\mathrm{SRT}}\right)}{\left(1+K_{\mathrm{TNN20}}\times\theta_{K_{\mathrm{TNN}}}^{T-20}\times\frac{f_{\mathrm{FNA}}}{K\ddot{\boldsymbol{\epsilon}}_{\mathrm{IFNA}}}\right)} - \sqrt{\left(\frac{\mu_{max20}\times\theta_{\mu}^{T-20}\times \mathrm{DO}}{\left(1+\frac{\mathrm{FA}}{K\ddot{\boldsymbol{\epsilon}}_{\mathrm{IFA}}}\right)\times(K_{\mathrm{O}}+\mathrm{DO})} - \left(b_{20}\times\theta_{b}^{T-20}+\frac{1}{\mathrm{SRT}}\right)\left(1+K_{\mathrm{TNN20}}\times\theta_{K_{\mathrm{TNN}}}^{T-20}\times\frac{f_{\mathrm{FNA}}}{K\ddot{\boldsymbol{\epsilon}}_{\mathrm{IFNA}}}\right)\right)^{2} - 4\times\left(b_{20}\times\theta_{b}^{T-20}+\frac{1}{\mathrm{SRT}}\right)^{2}\times K_{\mathrm{TNN20}}\times\theta_{K_{\mathrm{TNN}}}^{T-20}\times\frac{f_{\mathrm{FNA}}}{K\ddot{\boldsymbol{\epsilon}}_{\mathrm{IFNA}}}}}{2\times\left(b_{20}\times\theta_{b}^{T-20}+\frac{1}{\mathrm{SRT}}\right)\times\frac{f_{\mathrm{FNA}}}{K\ddot{\boldsymbol{\epsilon}}_{\mathrm{IFNA}}}} \quad (23)$$

$$\mathrm{TNN_{max}} = \frac{\frac{\mu_{max20}\times\theta_{\mu}^{T-20}\times \mathrm{DO}}{\left(1+\frac{\mathrm{FA}}{K\ddot{\boldsymbol{\epsilon}}_{\mathrm{1FA}}}\right)\times(K_{\mathrm{O}}+\mathrm{DO})} - \left(b_{20}\times\theta_{b}^{T-20}+\frac{1}{\mathrm{SRT}}\right)}{\left(1+K_{\mathrm{TNN20}}\times\theta_{K_{\mathrm{TNN}}}^{T-20}\times\frac{f_{\mathrm{FNA}}}{K\ddot{\boldsymbol{\epsilon}}_{\mathrm{1FNA}}}\right)} + \sqrt{\left(\frac{\mu_{max20}\times\theta_{\mu}^{T-20}\times \mathrm{DO}}{\left(1+\frac{\mathrm{FA}}{K\ddot{\boldsymbol{\epsilon}}_{\mathrm{1FA}}}\right)\times(K_{\mathrm{O}}+\mathrm{DO})} - \left(b_{20}\times\theta_{b}^{T-20}+\frac{1}{\mathrm{SRT}}\right)\left(1+K_{\mathrm{TNN20}}\times\theta_{K_{\mathrm{TNN}}}^{T-20}\times\frac{f_{\mathrm{FNA}}}{K\ddot{\boldsymbol{\epsilon}}_{\mathrm{1FNA}}}\right)\right)^{2} - 4\times\left(b_{20}\times\theta_{b}^{T-20}+\frac{1}{\mathrm{SRT}}\right)^{2}\times K_{\mathrm{TNN20}}\times\theta_{K_{\mathrm{TNN}}}^{T-20}\times\frac{f_{\mathrm{FNA}}}{K\ddot{\boldsymbol{\epsilon}}_{\mathrm{1FNA}}}}}{2\times\left(\mathrm{b}_{20}\times\theta_{\mathrm{b}}^{T-20}+\frac{1}{\mathrm{SRT}}\right)\times\frac{f_{\mathrm{FNA}}}{K\ddot{\boldsymbol{\epsilon}}_{\mathrm{1FNA}}}} \quad (24)$$

For AOB, using the relationship between TAN and FA of Eq. 9, $\mathrm{TAN_{min}}$ and $\mathrm{TAN_{max}}$ can be derived as Eqs. 25 and 26, respectively.

$$\mathrm{TAN_{min}} = FA_{\mathrm{min}}\times\frac{14}{17}\times\frac{\left[\exp\left(\frac{6344}{273+\mathrm{T}}\right)+10^{pH}\right]}{10^{pH}} \quad (25)$$

$$\mathrm{TAN_{max}} = FA_{\mathrm{max}}\times\frac{14}{17}\times\frac{\left[\exp\left(\frac{6344}{273+\mathrm{T}}\right)+10^{pH}\right]}{10^{pH}} \quad (26)$$

Modeling simulations

Simulations were conducted based on Eqs. 19–24 using six cases to evaluate the effect of pH, temperature, and SRT on a CSTR without biomass recycle. The kinetic parameter values used for modeling are summarized in Table 1 while the simulation conditions are presented in Table 2.

Results and discussion

Impact of pH: cases 1 and 2

Figure 1a, b shows the DO MSC curves for AOB and NOB at different pHs. Generally, if the operating DO is above the $\mathrm{DO_{min}}$ curves for AOB and/or NOB, the conditions support the growth of AOBs, NOBs, or both. FA inhibition increases with pH increase while FNA inhibition increases with pH decrease. For AOB, when the TAN concentration is below $\mathrm{TAN_{min}}$ or over $\mathrm{TAN_{max}}$, $\mathrm{DO_{min}}$ approaches infinity, which identifies the washout range (WR) for AOBs. Similar boundaries of $\mathrm{TNN_{min}}$ or over $\mathrm{TNN_{max}}$ also exist for NOB.

Case 1 simulates the effect of pH on AOB and NOB at a constant TNN concentration of 50 mg N/L and TAN concentration of 0–1000 mg N/L. At pH 7, AOB and NOB curves intersect at 38 mg N/L, implying that below 38 mg N/L, it is impossible to wash out NOB and maintain AOB by DO control as $\mathrm{DO_{min}}$ for NOB is lower than $\mathrm{DO_{min}}$ for AOB. The intersection TAN concentrations at pH 7.5, 8, 8.5, and 9 are 10, 3, 0, and 0 mg N/L, implying that the minimum operational TAN concentration decreases as pH increases. Both $\mathrm{TAN_{min}}$ and $\mathrm{TAN_{max}}$ concentrations for AOB decrease as pH increases. For example, for pH in the 7 to 9 range, the $\mathrm{TAN_{min}}$ concentration for AOB decreases from 24 to 0.3 mg N/L. Similarly, the $\mathrm{TAN_{max}}$ values for AOB at pH 7 and 7.5 are over 1000 mg N/L and at 8, 8.5, and 9 are approximately 489, 200, and 90 mg N/L. Due to FA inhibition, the $\mathrm{TAN_{max}}$ for NOB also decreases from 126 mg N/L at pH 7 to 0.3 mg N/L at pH 9. In this analysis, both $\mathrm{TAN_{min}}$ and $\mathrm{TAN_{max}}$ represent the TAN concentration at which $\mathrm{DO_{min}}$ reaches 5 mg /L. When the DO is 2 mg/L and TNN concentration is constant at 50 mg N/L, the TAN concentration range for shortcut nitrification at pH 7, 7.5, 8, 8.5, and 9 are 74–1000, 43–1000, 16–489, 5–200, and 1–90 mg N/L, respectively. Yan and Hu (2009) operated a CSTR at SRTs of 1 to 2 days, DO of 2 mg/L, temperature of 35 °C, pH 8, and achieved nitrite accumulation at a TAN of 150 and TNN of 180 mg N/L for CSTR. The computed $\mathrm{DO_{min}}$ for AOB growth and complete NOB washout based on this

Table 1 Various kinetic parameters selected for the model simulations of modified Park's model (at 20 °C)

	Kinetic parameters	AOB	NOB	Reference
K_S	Half-max-rate concentration (mg N/L)	0.75 (NH_3-N)	2.7 (TNN)	Park et al. (2010a); Van Hulle et al. (2007); Schramm et al. (1999)
K_O	Half-max-rate concentration (mg DO/L)	0.51	1.98	
μ_{max}	Maximum growth rate(day^{-1})	0.9	1.0	Metcalf&Eddy (2014)
b	decay coefficient (day^{-1})	0.17	0.17	
W	pH range	3.2	2.4	Park and Bae (2009)
pH_{opt}	Optimal pH	8.4	7.7	
θ_{Ks}	Temperature coefficient for Ks	1.029	1.029	Metcalf&Eddy (2003)
θ_{μ}	Temperature coefficient for μ_{max}	1.072	1.063	
θ_b	Temperature coefficient for b	1.04	1.04	
K_{IFA}	Inhibition concentration (mgFA/L)	10	0.75	Park et al. (2010a)
K_{IFNA}	Inhibition concentration (mgFNA/L)	0.5	0.1	

model for the conditions of Yan and Hu (2009) are 0.29–0.78 mg/L which are less than 2 mg/L and consistent with the experimental results.

Case 2 simulates the effect of pH on AOB and NOB at a constant TAN concentration of 50 mg N/L and TNN concentration of 0–1000 mg N/L (Fig. 1b). The DO_{min} for NOB are always higher than those for AOB, implying that shortcut nitrification is achievable at any pH, especially at pH over 8, when DO_{min} for NOB goes to infinity meaning that NOB are always washed out. The optimal pH is around 8 as the DO_{min} range for AOB with TNN ranging from 0 to 1000 mg/L are 0.15–0.17 mg/L at pH 8, 0.24–0.26 mg/L at pH 8.5, and 0.66–0.68 mg/L at pH 9. TNN concentrations exert minimal impact on the DO_{min} for AOB. As apparent from cases 1 and 2, the TAN has a much greater effect on the DO_{min} of AOB and NOB than the TNN. There is a turning point which corresponds to the minima of the DO_{min} curves (Fig. 1b as an example) on the TAN-DO curve for AOB and on the TNN-DO curve for NOB, when TNN or TAN is fixed. For example, in Fig. 1a, when TAN is lower than the turning point value, DO_{min} for AOB will increase significantly with TAN decrease. As discussed above, pH 8 seems to be optimal for AOB at constant TAN values at 50 mg N/L. However, the optimal pH may not be applicable to specific circumstances. For example, if an effluent TAN of 800 mg N/L and TNN of 50 mg N/L is required, only pH 7 or 7.5 can be utilized.

Impact of temperature: cases 3 and 4

The effect of temperature in the 10 to 35 °C range on the DO MSC curves for AOB and NOB is shown in Fig. 1c, d. Case 3 is similar to case 1 at a constant TNN concentration of

Table 2 Operational conditions for six simulation cases

Case	TAN (mg N/L)	TNN (mg N/L)	pH	Temperature (°C)	SRT (day)
1	0–1000	50	7, 7.5, 8, 8.5, 9	35	Infinity
2	50	0–1000	7, 7.5, 8, 8.5, 9	35	Infinity
3	0–1000	50	8	10, 15, 20, 25, 30, 35	Infinity
4	50	0–1000	8	10, 15, 20, 25, 30, 35	Infinity
5	0–1000	50	8	35	5, 10, 20, 30, infinity
6	50	0–1000	8	35	5, 10, 20, 30, infinity

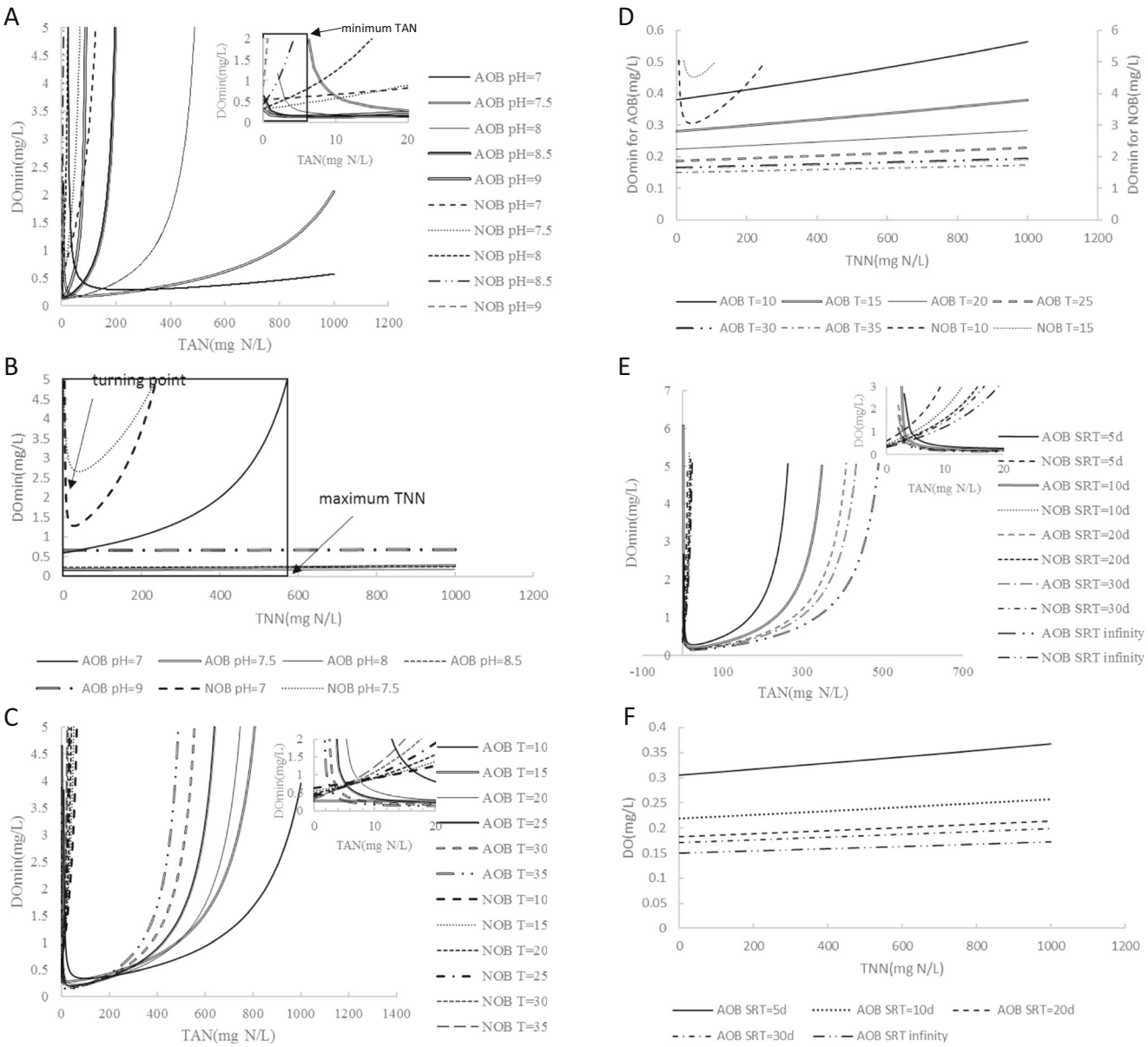

Fig. 1 Comparison with MSC curves (A–F represent case 1–6, respectively)

50 mg N/L and TAN concentration of 0–1000 mg N/L, while case 4 is similar to case 2 at a constant TAN concentration of 50 mg N/L and TNN concentration of 0–1000 mg N/L.

In case 3, both TAN_{min} and TAN_{max} values for AOB decreased as temperature increased. The TAN_{min} and TAN_{max} values for AOB decreased from 11 mg N/L and over 1000 mg N/L at 10 °C to 1.5 and 489 mg N/L at 35 °C. The TAN_{max} for NOB also decreased from 65 mg N/L at 10 °C to 24 mg N/L at 35 °C. The intersection TAN concentration of AOB and NOB curves decreased from 16 mg N/L at 10 °C to 3 mg N/L at 35 °C. From the aforementioned point of intersection to TAN_{max} for AOB, it is possible to maintain AOB and wash out NOB by adopting specific DO control. For example, from TAN_{max} for NOB to TAN_{max} for AOB, nitrite accumulation can always be achieved with DO higher than DO_{min} for AOB. In case 4, when TAN is fixed at 50 mg N/L, the DO_{min} for NOB are always higher than that for AOB, meaning that shortcut nitrification is achievable at any temperature in the 10 to 35 °C range.

Impact of SRT: cases 5 and 6

The effect of SRT on DO MSC curves for AOB and NOB is shown in Fig. 1e, f by changing SRT from 5 days to infinity while maintaining pH and temperature constant at 8 and 35 °C, respectively.

Case 5 simulates the effect of SRT on AOB and NOB at a constant TNN concentration of 50 mg N/L and TAN concentration of 0–1000 mg N/L. The TAN_{min} concentrations for AOB at any SRT are lower than 3 mg N/L. Both TAN_{max} values for AOB and NOB increased with SRT. The TAN_{max} concentration for AOB increases from 263 mg N/L at an SRT of 5 days to 489 mg N/L at an infinite SRT. The TAN_{max} for NOB increased from 13 mg N/L at an SRT of 5 days to 24 mg N/L at an infinite SRT. The intersection point of the DO curves for AOB and NOB corresponds to the TAN concentration at which both species survive. The common TAN concentration for both AOB and NOB decreased as SRT increased from 5 days to infinity but always fell within the range of 3 to 4 mg N/L.

Case 6 simulates the effect of SRT on AOB at a constant TAN concentration of 50 mg N/L and TNN concentration of 0–1000 mg N/L. At all SRTs, NOB will be washed out, ending up with nitrite accumulation when DO is higher than DO_{min} for AOB. From Fig. 1f, DO_{min} for AOB decreased as SRT increased at a given TNN concentration.

Special applications of the DOMSC curves

Recently, the feasibility and performance of nitrification-anammox system at low nitrogen concentrations (20 to 60 mg NH_4-N/L) and low temperatures (5–25 °C) (De Clippeleir et al. 2013; Hu et al. 2013; Lotti et al. 2014; Persson et al. 2014) has elicited the attention of both researchers and practitioners. The MSC curves for various pHs for the special case of shortcut nitrification-anammox process at 10 °C are shown in Fig. 2. In this simulation, SRT were set at 10, 20, and 30 days, temperature was set as 10, 15, and 20 °C, and pH was set at 8. Stoichiometrically, anammox needs an influent that has almost the same concentrations of ammonium- and nitrite-nitrogen (Strous et al. 1997). Thus, the TAN/TNN was set at 1:1.32 with TN as the sum of TAN and TNN, i.e., completely ignoring nitrates. As presented in Fig. 2, the DO_{min} for both AOB and NOB decreased when SRT or temperature increased. The minimum SRT decreased with temperature increase. At a given condition, for example, a TN of 60 mg N/L, pH 8, the minimum SRT was 13 days at 10 °C, decreasing to 7 days at 15 °C, and further to 3.6 days at 35 °C.

Analysis of literature results with the MSC model

Table 3 summarizes the comparison of literature operational conditions and performance data with the computed DO_{min} values based on this model. Columns 1 to 8 are from the experimental data; columns 10 to 11 are AOB and NOB DO_{min} values calculated using the experimental values in this model. It can be seen that almost all experimental DO values are higher than DO_{min} for AOB and lower than DO_{min} for NOB, suggesting that this model may become a predictive tool for successful shortcut nitrification system.

When analyzing the effect of SRT in this work, SRT ranged from 5 to 30 days. However, the SHARON

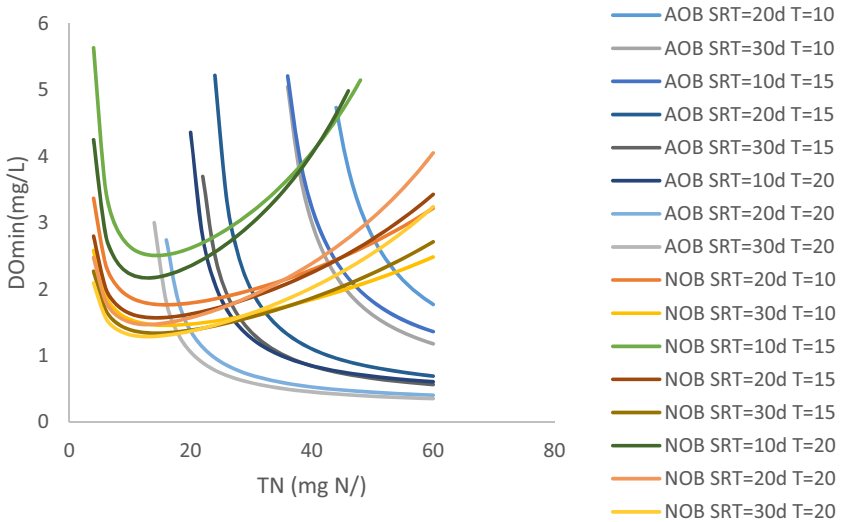

Fig. 2 DO_{min} curves by SRT(10–30 days) and temperature(10–20 °C) for shortcut nitrification to provide an input to the ANAMMOX process

Table 3 Determination of the minimum DO concentration in shortcut nitrification systems

Reference	TAN (mg N/L)	TNN (mg N/L)	pH	T (°C)	NO_2/NO_x (%)	SRT (day)	DO (mg/L)	Duration (day)	System	DO_{min}	
										AOB	NOB
Column number	1	2	3	4	5	6	7	8	9	10	11
Chung et al. (2007)	250	170	8	30	93	31	<2	800	Activated sludge with biofilm carriers and a clarifier	0.66	WR
Galí et al. (2007b)	350	350	6.5–6.7	35	>90	1	3	180	SHARON	WR	WR
van Dongen et al. (2001)	550	600	6.4–7	30–40	100	1	NA	250	SHARON	WR	WR
Fux et al. (2004)	400	400	6.2–7	30	94	Infinity	2–4	90	Moving bed biofilm reactor	0.73-WR	WR
Chen et al. (2010)	137.3	353.9	8	30	95.7	8–12	>1.5	70	Continuous stirred-tank reactor	2.55–4.25	WR
	73.2	391.4	7–7.5	30	85.3	14–18	>1	55	Continuous stirred-tank reactor	0.48-WR	WR
Sinha and Annachhatre (2007)	127.5	154.2	8	35	81	12–14	0.3–0.5	120	Continuous stirred-tank reactor with a settler	0.37–0.39	WR
Chuang et al. (2007)	50	45	7.6	30	>90	Infinity	0.2	150	Closed down-flow hanging sponge reactor	0.20	2.67
Ruiz et al. (2006)	12	390	7.8–7.9	30	67	Infinity	0.7	50	Activated sludge reactor with a settler	0.27–0.34	1.24–1.38
Ciudad et al. (2005)	30	400	7.8	25	80	Infinity	1.4	300	Activated sludge reactor with a settler	0.27	3.29
Park et al. (2010b)	80	163	8.2	30	98	20–25	1.3 ± 0.3	96	Suspended growth shortcut biological nitrogen removal with a clarifier	0.30–0.31	WR

process usually has an SRT less than 2 days (Galí et al. 2007a; van Dongen et al. 2001; Hellinga et al. 1998). As apparent from Table 3, this model was unable to predict the SHARON process (Galí et al. 2007b; van Dongen et al. 2001) as the DO_{min} for AOB by the model suggested that the AOB would be washed out under the Sharon conditions. The reason for the aforementioned discrepancy is different kinetics. The maximum observed growth rates of AOB in the SBR and SHARON were 1.0 and 2.0, and 1.3 and 2.4 day^{-1} in the study of Galí et al. (2007a) and Galí et al. (2007b), respectively. One set of SHARON kinetic parameters for AOB determined by Van Hulle et al. (2007) at pH 7 and a temperature of 35 °C is as follows: b = 0.045 day^{-1}, K_{NH3} = 0.75 $mgNH_3$-N L^{-1}, K_{INH3} was very high and K_{IHNO2} = 2.04 $mgHNO_2$-N L^{-1} and Ko = 0.94 mg/L. By using the aforementioned kinetic parameters and μ_{max} of 2.4 day^{-1}, the predicted DO_{min} for AOB was 1.09 to 1.36 mg/L in the case of van Dongen et al. (2001). The model predictions for several typical Sharon processes are shown in Table 4. Although in some studies the actual DO was not mentioned, the model suggested that the AOB could survive with DO higher than DO_{min} while NOB would be washed at any operational DO. This indicates that the model could predict the SHARON process based on its specific kinetic parameters. In this study, b of 0.17 day^{-1} at 20 °C and θ_b of 1.04 were used, resulting in b value of 0.31 day^{-1} at 35 °C, which is actually higher than the b value of 0.23 day^{-1} at 35 °C reported by Magri et al. (2007). In fact, the reported b values at 35 °C range from 0.045 to 0.31 day^{-1}(Henze et al. 1987; Metcalf&Eddy 2003; Van Hulle et al. 2007; Liu et al. 2016). In addition, the FA and FNA inhibition threshold concentrations range from 5.0 to 27.3 mg FA/L, and 0.09 to 0.97 mg FNA/L (Park and Bae 2009).

Model use for bioreactor design

This model not only suggests a DO range in which nitrite accumulation can be successfully achieved, but also provides bioreactor design information such as SRT.

For example, if a CSTR is to be designed to treat wastewater with Q_{in}, influent TAN of 220 mg N/L to achieve an effluent concentration of TAN 20 mg N/L and TNN 200 mg N/L at a pH of 7.5 and a temperature of 35 °C, the SRT ranges from 2.4 days to infinity. Furthermore, the operational DO ranges from 0.31 to 1.19 mg/L at infinite SRT to over 4.5 mg/L at an SRT of 2.4 days.

Table 4 Model prediction of Sharon reactors based on specific kinetic values

Reference	TAN (mg N/L)	TNN (mg N/L)	pH	T (°C)	NO_2/NO_x (%)	SRT (day)	DO (mg/L)	DO_{min}	
								AOB	NOB
Galí et al. (2007b)	350	350	6.5–6.7	35	>90	1	3	2–2.86	WR
van Dongen et al. (2001)	550	600	6.4–7	30–40	100	1	NA	1.09–1.36	WR
Galí et al. (2007a)	350	400	7	35	88	1.4	3	0.65	WR
Hellinga et al. (1998)	130	345	7.4	35	100	1.5	NA	1.05	WR

Conclusions

A model for successful shortcut nitrification conditions determination was derived based on MSC values. In addition, the effect of temperature, pH, and SRT was analyzed. Specific application of this model for shortcut nitrification coupled with anaerobic ammonium oxidation (ANAMMOX), in which the effluent concentrations of nitrite and ammonium from shortcut nitrification were equal, was discussed. Comparison of the model predicted DO_{min} with experimental data suggested that this model can be a useful and practical tool for shortcut nitrification systems design and operation.

Acknowledgements This work was supported by the National Science and Engineering Research council of Canada [grant number CRDPJ 458990-13].

References

Anthonisen A, Loehr R, Prakasam T, Srinath E (1976) Inhibition of nitrification by ammonia and nitrous acid. Journal (Water Pollution Control Federation) 48:835–852

Beccari M, Passino R, Ramadori R, Tandoi V (1983) Kinetics of dissimilatory nitrate and nitrite reduction in suspended growth culture. Journal Water Pollution Control Federation 55:58–64

Boon B, Laudelout H (1962) Kinetics of nitrite oxidation by *Nitrobacter winogradskyi*. Biochem J 85:440

Chen JW, Zheng P, Yu Y, Mahmood Q, Tang CJ (2010) Enrichment of high activity nitrifers to enhance partial nitrification process. Bioresour Technol 101(19):7293–7298

Chuang HP, Ohashi A, Imachi H, Tandukar M, Harada H (2007) Effective partial nitrification to nitrite by down-flow hanging sponge reactor under limited oxygen condition. Water Res 41(2):295–302

Chung J, Bae W, Lee YW, Rittmann BE (2007) Shortcut biological nitrogen removal in hybrid biofilm/suspended growth reactors. Process Biochem 42(3):320–328

Ciudad G, Rubilar O, Munoz P, Ruiz G, Chamy R, Vergara C, Jeison D (2005) Partial nitrification of high ammonia concentration wastewater as a part of a shortcut biological nitrogen removal process. Process Biochem 40(5):1715–1719

De Clippeleir H, Vlaeminck SE, De Wilde F, Daeninck K, Mosquera M, Boeckx P, Verstraete W, Boon N (2013) One-stage partial nitritation/anammox at 15 °C on pretreated sewage: feasibility demonstration at lab-scale. Appl Microbiol Biotechnol 97:10199–10210

Fux C, Huang D, Monti A, Siegrist H (2004) Difficulties in maintaining long-term partial nitritation of ammonium-rich sludge digester liquids in a moving-bed biofilm reactor (MBBR). Water Sci Technol 49(11–12):53–60

Galí A, Dosta J, van Loosdrecht MCM, Mata-Alvarez J (2006) Biological nitrogen removal via nitrite of reject water with a SBR and chemostat SHARON/denitrification process. Ind Eng Chem Res 45(22):7656–7660

Galí A, Dosta J, Mace S, Mata-Alvarez J (2007a) Comparison of reject water treatment with nitrification/denitrification via nitrite in SBR and SHARON chemostat process. Environ Technol 28(2):173–176

Galí A, Dosta J, van Loosdrecht MCM, Mata-Alvarez J (2007b) Two ways to achieve an anammox influent from real reject water treatment at lab-scale: partial SBR nitrification and SHARON process. Process Biochem 42:715–720

Guo JH, Peng YZ, Wang SY, Zheng YN, Huang HJ, Ge SJ (2009) Effective and robust partial nitrification to nitrite by real-time aeration duration control in an SBR treating domestic wastewater. Process Biochem 44:979–985

Hellinga C, Schellen A, Mulder J, Van Loosdrecht M, Heijnen J (1998) The SHARON process: an innovative method for nitrogen removal from ammonium-rich waste water. Water Sci Technol 37:135–142

Hellinga C, Van Loosdrecht M, Heijnen J (1999) Model based design of a novel process for nitrogen removal from concentrated flows. Math Comput Model Dyn Syst 5:351–371

Henze M, Grady Jr C, Gujer W, Marais G, Matsuo T (1987) Activated Sludge Model No. 1: IAWPRC Scientific and Technical Report No. 1. IAWPRC, London

Hu Z, Lotti T, de Kreuk M, Kleerebezem R, van Loosdrecht M, Kruit J, Jetten MS, Kartal B (2013) Nitrogen removal by a nitritation-anammox bioreactor at low temperature. Appl Environ Microbiol 79:2807–2812

Liu X, Kim M, Nakhla G (2016) Operational conditions for successful partial nitrification in an SBR based on process kinetics. Environ Technol (just-accepted), 1–27. doi:10.1080/09593330.2016.1209246

Lotti T, Kleerebezem R, Hu Z, Kartal B, Jetten M, van Loosdrecht M (2014) Simultaneous partial nitritation and anammox at low temperature with granular sludge. Water Res 66:111–121

Magri A, Corominas L, Lopez H, Campos E, Balaguer M, Colprim J, Flotats X (2007) A model for the simulation of the SHARON process: pH as a key factor. Environ Technol 28:255–265

Metcalf&Eddy (2014) Wastewater Engineering: Treatment and Resource Recovery. McGraw-Hill international ed.

Metcalf&Eddy (2003) Wastewater engineering: treatment, disposal, reuse, 4th edn. Inc., McGraw-Hill, New York

Park S, Bae W, Chung J, Baek S-C (2007) Empirical model of the pH dependence of the maximum specific nitrification rate. Process Biochem 42:1671–1676

Park S, Bae W (2009) Modeling kinetics of ammonium oxidation and nitrite oxidation under simultaneous inhibition by free ammonia and free nitrous acid. Process Biochem 44:631–640

Park S, Bae W, Rittmann BE (2010a) Operational boundaries for nitrite accumulation in nitrification based on minimum/maximum substrate concentrations that include effects of oxygen limitation, pH,

and free ammonia and free nitrous acid inhibition. Environmental Science & Technology 44(1):335–342

Park S, Bae W, Rittmann BE, Kim S, Chung J (2010b) Operation of suspended-growth shortcut biological nitrogen removal (SSBNR) based on the minimum/maximum substrate concentration. Water Res 44(5):1419–1428

Persson F, Sultana R, Suarez M, Hermansson M, Plaza E, Wilén B-M (2014) Structure and composition of biofilm communities in a moving bed biofilm reactor for nitritation–anammox at low temperatures. Bioresour Technol 154:267–273

Rittmann BE, McCarty PL (1980) Model of steady-state-biofilm kinetics. Biotechnol Bioeng 22:2343–2357

Rittmann BE, McCarty PL (2001) Environmental biotechnology: principles and applications. McGraw-Hill

Ruiz G, Jeison D, Rubilar O, Ciudad G, Chamy R (2006) Nitrification-denitrification via nitrite accumulation for nitrogen removal from wastewaters. Bioresour Technol 97(2):330–335

Schramm A, de Beer D, van den Heuvel JC, Ottengraf S, Amann R (1999) Microscale distribution of populations and activities of Nitrosospira and Nitrospira spp. along a macroscale gradient in a nitrifying bioreactor: quantification by in situ hybridization and the use of microsensors. Appl Environ Microbiol 65(8):3690–3696

Sinha B, Annachhatre AP (2007) Assessment of partial nitrification reactor performance through microbial population shift using quinone profile, FISH and SEM. Bioresour Technol 98(18):3602–3610

Strous M, Van Gerven E, Zheng P, Kuenen JG, Jetten MS (1997) Ammonium removal from concentrated waste streams with the anaerobic ammonium oxidation (anammox) process in different reactor configurations. Water Res 31:1955–1962

Turk O, Mavinic DS (1987) Benefits of using selective-inhibition to remove nitrogen from highly nitrogenous wastes. Environ Technol Lett 8:419–426

Vadivelu VM, Keller J, Yuan Z (2006) Effect of free ammonia and free nitrous acid concentration on the anabolic and catabolic processes of an enriched Nitrosomonas culture. Biotechnol Bioeng 95:830–839

van Dongen U, Jetten MSM, van Loosdrecht MCM (2001) The SHARON((R))-anammox((R)) process for treatment of ammonium rich wastewater. Water Sci Technol 44:153–160

Van Hulle SW, Volcke EI, Teruel JL, Donckels B, van Loosdrecht M, Vanrolleghem PA (2007) Influence of temperature and pH on the kinetics of the Sharon nitritation process. J Chem Technol Biotechnol 82:471–480

van Kempen R, Mulder JW, Uijterlinde CA, Loosdrecht MCM (2001) Overview: full scale experience of the SHARON (R) process for treatment of rejection water of digested sludge dewatering. Water Sci Technol 44:145–152

Van Loosdrecht MCM, Jetten MSM (1998) Microbiological conversions in nitrogen removal. Water Sci Technol 38:1–7

Yan J, Hu YY (2009) Comparison of partial nitrification to nitrite for ammonium-rich organic wastewater in sequencing batch reactors and continuous stirred-tank reactor at laboratory-scale. Water Sci Technol 60:2861–2868